Regulatory T Cells Reduce Acute Lung Injury Fibroproliferation by Decreasing Fibrocyte Recruitment

Brian T. Garibaldi[1], Franco R. D'Alessio[1], Jason R. Mock[1], D. Clark Files[1,2], Eric Chau[1], Yoshiki Eto[1], M. Bradley Drummond[1], Neil R. Aggarwal[1], Venkataramana Sidhaye[1], and Landon S. King[1]

[1]Division of Pulmonary and Critical Care Medicine, Johns Hopkins Asthma and Allergy Center, Johns Hopkins University School of Medicine, Baltimore, Maryland; and [2]Pulmonary, Critical Care, Allergy and Immunology Division, Department of Internal Medicine, Wake Forest University School of Medicine, Winston-Salem, North Carolina

Acute lung injury (ALI) causes significant morbidity and mortality. Fibroproliferation in ALI results in worse outcomes, but the mechanisms governing fibroproliferation remain poorly understood. Regulatory T cells (Tregs) are important in lung injury resolution. Their role in fibroproliferation is unknown. We sought to identify the role of Tregs in ALI fibroproliferation, using a murine model of lung injury. Wild-type (WT) and lymphocyte-deficient *Rag-1*$^{-/-}$ mice received intratracheal LPS. Fibroproliferation was characterized by histology and the measurement of lung collagen. Lung fibrocytes were measured by flow cytometry. To dissect the role of Tregs in fibroproliferation, *Rag-1*$^{-/-}$ mice received CD4^{+}CD25^{+} (Tregs) or CD4^{+} CD25^{-} Tcells (non-Tregs) at the time of LPS injury. To define the role of the chemokine (C-X-C motif) ligand 12 (CXCL12)–CXCR4 pathway in ALI fibroproliferation, *Rag-1*$^{-/-}$ mice were treated with the CXCR4 antagonist AMD3100 to block fibrocyte recruitment. WT and *Rag-1*$^{-/-}$ mice demonstrated significant collagen deposition on Day 3 after LPS. WT mice exhibited the clearance of collagen, but *Rag-1*$^{-/-}$ mice developed persistent fibrosis. This fibrosis was mediated by the sustained epithelial expression of CXCL12 (or stromal cell-derived factor 1 [SDF-1]) that led to increased fibrocyte recruitment. The adoptive transfer of Tregs resolved fibroproliferation by decreasing CXCL12 expression and subsequent fibrocyte recruitment. Blockade of the CXCL12–CXCR4 axis with AMD3100 also decreased lung fibrocytes and fibroproliferation. These results indicate a central role for Tregs in the resolution of ALI fibroproliferation by reducing fibrocyte recruitment along the CXCL12–CXCR4 axis. A dissection of the role of Tregs in ALI fibroproliferation may inform the design of new therapeutic tools for patients with ALI.

Keywords: acute lung injury; fibroproliferative ARDS; fibrocytes; regulatory T cells; lung injury resolution

Acute lung injury (ALI) and acute respiratory distress syndrome (ARDS) affect 190,000 individuals in the United States each year, accounting for 75,000 deaths (1). The only treatment that improves outcomes involves a lung-protective strategy in patients on mechanical ventilation (2). Mortality from ALI/ARDS remains as high as 44% (3).

CLINICAL RELEVANCE

Fibroproliferation in the context of acute lung injury (ALI) leads to worse outcomes, but the factors that underlie the fibroproliferative phase of ALI remain unknown. We have shown that regulatory T cells reduce fibroproliferation after LPS-induced ALI by reducing fibrocyte recruitment to the lung along the CXCL12–CXCR4 axis. This may lead to the development of novel diagnostic and therapeutic strategies for patients with ALI.

ALI/ARDS is divided into an exudative phase marked by edema fluid, hyaline membrane formation, and neutrophilic infiltration, followed in some patients by a fibroproliferative phase (4). Fibroproliferation is part of the normal repair response, and is characterized by the intra-alveolar accumulation of fibroblasts and collagen deposition. If this process is ineffective or continues unabated, patients may develop fibrosis (5). Longer durations of ARDS correspond to increased lung collagen and fibrosis, and portend worse outcomes (6). Fibroproliferative changes on biopsy and computed tomography predict mortality (7, 8). The determinants of prolonged fibroproliferation and factors that govern its resolution remain poorly understood.

The fibroblast is a key cell in fibroproliferation (9). The source of activated fibroblasts (myofibroblasts) in ALI remains unclear. Three cell populations likely contribute: (*1*) resident lung fibroblasts (10), (*2*) epithelial cells that transform into myofibroblasts via epithelial-to-mesenchymal transition (11), and (*3*) bone marrow progenitors called fibrocytes. Fibrocytes are identified by their expression of CD45, collagen-1 (Col-1), and CXCR4 (12–14). In a model of bleomycin fibrosis, fibrocytes accounted for 20% of myofibroblasts (10, 15). Fibrocytes are contained in the bronchoalveolar lavage (BAL) and blood of patients with idiopathic pulmonary fibrosis (IPF), and may predict exacerbations (14, 16). Recently, fibrocytes were found in the BAL of patients with ARDS, and were associated with increased mortality (17, 18). The mechanisms governing fibrocyte recruitment and activation in ALI remain unknown.

Persistent inflammation is a hallmark of fibroproliferative ARDS (4). Our group has highlighted a central role for regulatory T cells (Tregs, i.e., CD4^{+}CD25^{+}Foxp3^{+} T cells) in the resolution of lung inflammation (19). The role of Tregs in the fibroproliferative response to ALI has not been described, to the best of our knowledge.

Using a well-established model of lung injury involving intratracheal LPS (20), we show that lymphocyte-deficient *Rag-1*$^{-/-}$ mice demonstrate persistent fibroproliferation, characterized by sustained fibrocyte recruitment to the lung. The adoptive transfer of Tregs, but not other CD4^{+} T cells, into *Rag-1*$^{-/-}$ mice reduces

(*Received in original form May 31, 2012 and in final form August 30, 2012*)

This work was supported by National Institutes of Health grant NRSA F32HL104908–02 (B.T.G.), National Institutes of Health grant K99HL103973 (F.D.R.), National Institutes of Health grant R01HL089346 (L.S.K.), and the Johns Hopkins Bayview Scholars Program (L.S.K.).

B.T.G., F.R.D., J.R.M., V.S., and L.S.K. conceived and designed experiments. B.T.G., F.R.D., D.C.F., J.R.M., E.C., Y.E., and N.R.A. performed experiments and analysis. M.B.D. provided assistance with statistical analysis. B.T.G. and L.S.K. wrote the manuscript and provided creative input.

Correspondence and requests for reprints should be addressed to Brian T. Garibaldi, M.D., Division of Pulmonary and Critical Care Medicine, Johns Hopkins Asthma and Allergy Center, Johns Hopkins University School of Medicine, 5501 Hopkins Bayview Circle, 4A-64, Baltimore, MD 21224. E-mail: bgariba1@jhmi.edu

This article has an online supplement, which is accessible from this issue's table of contents at www.atsjournals.org

Am J Respir Cell Mol Biol Vol 48, Iss. 1, pp 35–43, Jan 2013

Originally Published in Press as DOI: 10.1165/rcmb.2012-0198OC on September 20, 2012
Internet address: www.atsjournals.org

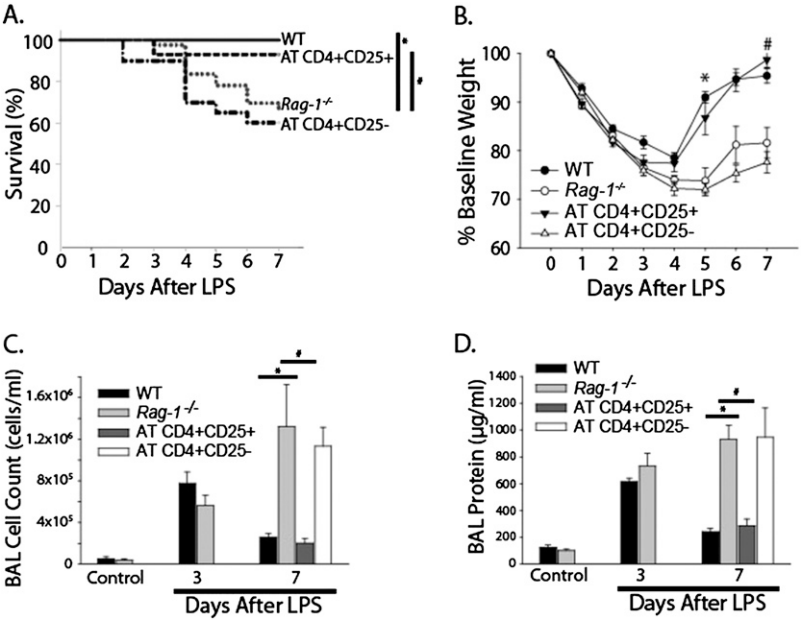

Figure 1. Adoptive transfer of T regulatory cells (Tregs; $CD4^+CD25^+$ cells) but not $CD4^+CD25^-$ cells into *Rag-1*$^{-/-}$ mice restored normal resolution of lung injury. (*A*) Survival curves after intratracheal LPS for all groups ($^*P = 0.021$ by survival log-rank, and $^{\#}P = 0.024$ by χ^2 test, $n \geq 14$ in all groups). (*B*) Weight loss presented as percentage of baseline weight after intratracheal LPS for all groups ($^*P < 0.001$, and $^{\#}P < 0.001$, $n \geq 14$, all groups). (*C*) Bronchoalveolar lavage (BAL) cell counts on Day 3 and Day 7 after intratracheal LPS or intratracheal water for all groups ($^*P = 0.012$ and $^{\#}P < 0.05$, $n > 4$, all groups). (*D*) BAL protein measured by the method of Lowry on Day 3 and Day 7 after intratracheal LPS or intratracheal water for all groups ($^*P = 0.001$ and $^{\#}P = 0.006$, $n \geq 4$ all groups). AT, adoptive transfer; WT, wild-type.

fibrocyte number and resolves fibroproliferation. This fibrocyte reduction is caused by a Treg-mediated decrease in lung CXCL12, a chemokine that induces fibrocyte recruitment. Epithelial cells are an important source of CXCL12, suggesting that Tregs reduce CXCL12 concentrations by interacting with the epithelium. The blockade of CXCR4, the receptor for CXCL12, decreases fibrocyte numbers and fibroproliferation in *Rag-1*$^{-/-}$ mice, providing further evidence for the importance of the CXCL12–CXCR4 axis in ALI fibroproliferation. Our results indicate that Tregs play a critical role in the fibroproliferative response to ALI, and that targeting the CXCL12–CXCR4 pathway may provide new insights into the treatment of fibroproliferative ARDS.

Some of these results were previously reported in the form of an abstract (21).

MATERIALS AND METHODS

Mice

C57BL/6 wild-type (WT) and *Rag-1*$^{-/-}$ mice (aged 6–8 wk) were purchased from Jackson Laboratories (Bar Harbor, ME). Green-fluorescent protein (GFP)-labeled, $Foxp3^+$ mice were the gift of Alexander Rudensky (Sloan-Kettering Institute, New York, NY). Protocols were approved by the Johns Hopkins Animal Care and Use Committee (Baltimore, MD).

Preparation of Mice

Mice were anesthetized with intraperitoneal ketamine and acetylpromazine (150 and 13.5 mg/kg, respectively) before tracheal exposure. *Escherichia coli* LPS (3.75 μg/g, O55:B5 L2880; Sigma-Aldrich, St. Louis, MO) or sterile water was instilled intratracheally via 20-gauge catheter. Animals were killed by vena cava exsanguination (19).

CXCR4 Blockade

Rag-1$^{-/-}$ mice underwent daily intraperitoneal injections of AMD3100 (200 μg/250 μl PBS; Sigma-Aldrich) or PBS (250 μl).

Isolation and Adoptive Transfer of Tregs

$CD4^+CD25^+$ and $CD4^+CD25^-$ T cells were isolated from GFP-$Foxp3^+$ spleens using magnetic beads (Miltenyi, Cambridge, MA) (19). Single-cell suspensions (1×10^6 cells in 100 μl PBS) were transferred within 60 minutes after LPS by retro-orbital injection. Treg purity was measured at 85–90% by flow cytometry.

Analysis of BAL Fluid

Two aliquots of 0.7 ml PBS were instilled into the right lung. Cell counts were determined by hemocytometer. Protein was measured using the method of Lowry (19).

Lung Histology and Immunohistochemistry

Left lungs were inflated to 25 cm H_2O with 1% low-melting agarose (Invitrogen, Grand Island, NY) (19) for evaluation by Masson's trichrome. Sections were prepared for immunohistochemistry with anti–SDF-1 AB (1/50, clone 79018; R&D Systems, Minneapolis, MN), followed by a mouse-on-mouse immunodetection technique (Vector Laboratories, Burlingame, CA), peroxidase-conjugated secondary antibody, and development with 3,3-diaminobenzidine.

Lung and BAL Collagen Content

Left lungs were frozen in liquid nitrogen. Lungs were homogenized in 1 ml of Complete Lysis Buffer (Roche, Indianapolis, IN), using an Ultra-Turrax tissue homogenizer (Janke and Kunkel, Wilmington, NC). Collagen was measured by Sircol Assay (BioColor, Carrickfergus, UK), according to the manufacturer's instructions.

Lung CXCL12 Concentrations

CXCL12 concentrations were measured in lung homogenates, using an ELISA duoset (R&D Systems).

Preparation of Lung Homogenates for Flow Cytometry

Right lungs were excised, minced, and incubated at 37°C in RPMI containing 2.4 mg/ml collagenase I and 20 μg/ml DNase (Invitrogen), and then mashed through a 70-μm nylon strainer (BD Biosciences, San Jose, CA). For epithelial cell isolation, lungs were instilled with 1.2 ml Dispase (BD Biosciences), with 3 U/ml elastase (Worthington, Lakewood, NJ) at removal. Red blood cells were removed using ACK lysis buffer (Invitrogen), and cells were resuspended in FACS buffer.

Flow Cytometry

Cells were prepared for FACS analysis (19). Surface stains included Alexa-700 conjugated anti-CD4 (Ebioscience, San Diego, CA), allophycocyanin-conjugated (APC) anti-CXCR4 (BD Biosciences), APC-Cy7–conjugated anti-CD326, and biotinylated anti-CD45 and CD31 with V450-conjugated streptavidin secondary (Biolegend, San Diego, CA). Intracellular stains included biotinylated rabbit anti–Col-I

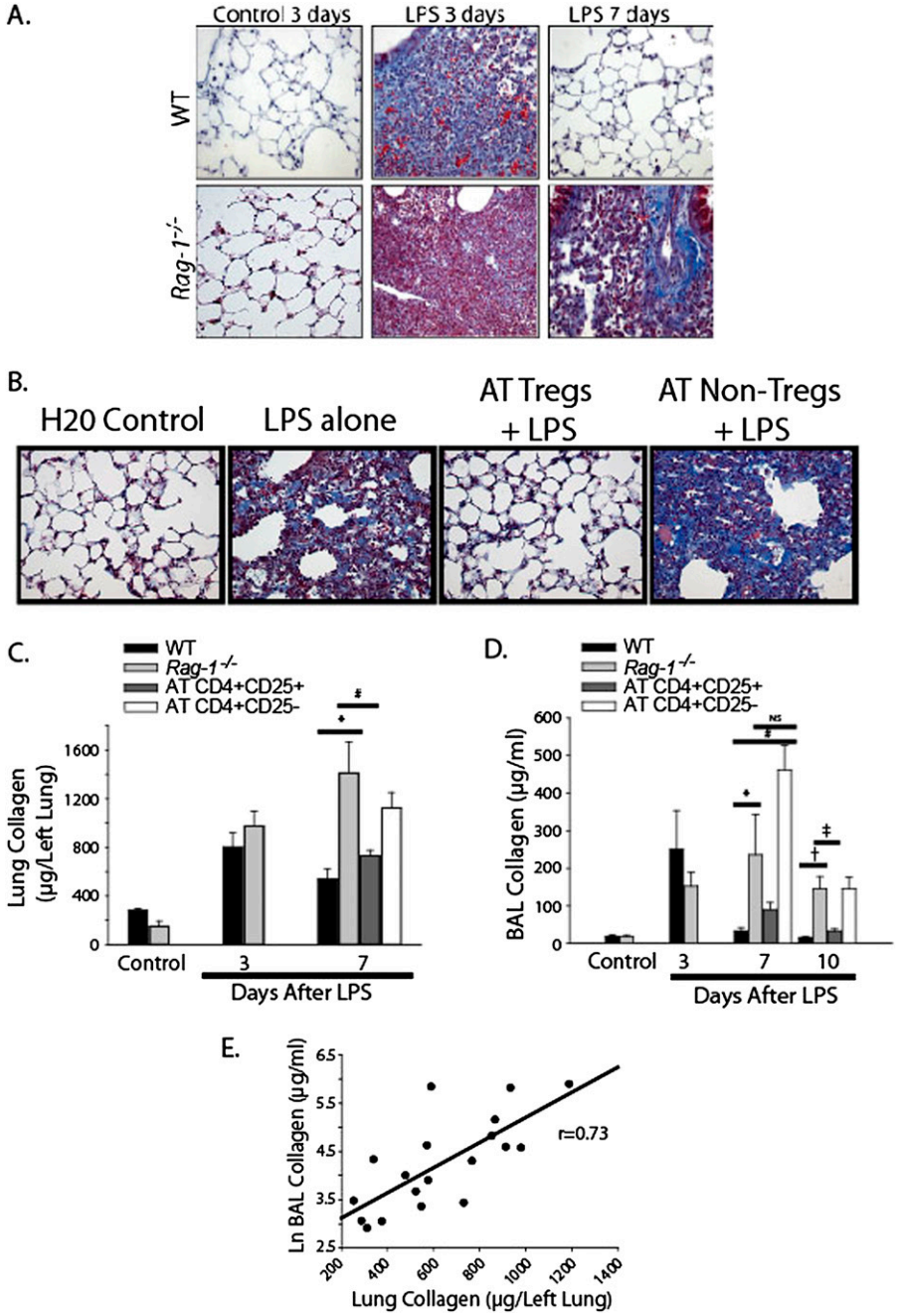

Figure 2. Adoptive transfer of Tregs reduced fibroproliferation in *Rag-1*$^{-/-}$ mice after LPS injury. (*A*) Lung sections were stained with Masson's trichrome to highlight collagen deposition on Day 3 and Day 7 after intratracheal LPS or intratracheal water in WT and *Rag-1*$^{-/-}$ mice ($n \geq 3$ in each group; images are of representative examples, ×200 magnification). (*B*) Lung sections were stained with Masson's trichrome on Day 7 after intratracheal LPS or intratracheal water in *Rag-1*$^{-/-}$ mice, *Rag-1*$^{-/-}$ mice + Tregs, and *Rag-1*$^{-/-}$ mice + non-Tregs (images are of representative examples, ×200 magnification, $n \geq 3$ in each group). (*C*) Lung collagen was measured by Sircol assay in all groups on Day 3 and Day 7 after intratracheal LPS ($^{*}P = 0.009$ and $^{\#}P = 0.047$, $n \geq 4$, all groups). (*D*) BAL collagen was measured by Sircol assay in all groups on Day 3, Day 7, and Day 10 after intratracheal LPS ($^{*}P = 0.002$, $^{\dagger}P = 0.003$, $^{\ddagger}P = 0.005$, and $^{\#}P = 0.005$, $n \geq 3$, all groups). (*E*) Lung collagen was positively correlated with the natural log of BAL collagen ($r = 0.73$, $P < 0.001$, using Pearson product moment correlation).

antibody (Rockland Chemicals, Gilbertsville, PA) with a PE–Texas red–conjugated streptavidin secondary (BD Biosciences) and APC-conjugated anti-CXCL12 (R&D Systems).

Statistical Analysis

Mortality was analyzed by χ^2 test. Markers of injury were compared using the Student *t* test or Mann-Whitney rank sum test. Multiple groups were compared using one-way ANOVA or one-way ANOVA on ranks. Pairwise comparisons were performed using the Student *t* test with the Bonferroni correction or the Dunn test. Lung CXCL12 was compared with fibrocyte numbers, using linear regression analysis on log-transformed data. Statistical analysis was performed using Sigmaplot 11.0 (Systat Software, Inc., Chicago, IL).

Further details on adoptive transfers, FACS, the Sircol assay, ELISA, and immunohistochemistry are provided in the online supplement.

RESULTS

Resolution of LPS-Induced Lung Injury Was Impaired in Lymphocyte-Deficient Mice

After the administration of intratracheal LPS, *Rag-1*$^{-/-}$ mice demonstrated increased mortality when compared with WT mice (Figure 1A). Both WT and *Rag-1*$^{-/-}$ mice lost body weight, but WT mice returned to near-baseline body weight by Day 7, whereas *Rag-1*$^{-/-}$ mice demonstrated persistently decreased body weight (Figure 1B). Both WT and *Rag-1*$^{-/-}$ mice exhibited similar degrees of lung injury on Day 3, as indicated by BAL cell count (Figure 1C) and protein (Figure 1D). Both BAL cell counts and protein returned to near baseline values by Day 7 in WT mice, whereas these remained elevated in *Rag-1*$^{-/-}$ mice (Figures 1C and 1D).

Adoptive Transfer of Tregs Restored Normal Resolution of Lung Injury

After magnetic bead isolation, Tregs ($CD4^+CD25^+$ cells; 90% $Foxp3^+$) or non-Tregs ($CD4^+CD25^-$ cells) were adoptively transferred into intratracheal LPS–exposed *Rag-1*$^{-/-}$ mice. The adoptive transfer of Tregs but not non-Tregs into *Rag-1*$^{-/-}$ mice 1 hour after intratracheal LPS restored the normal resolution of lung injury, as evidenced by significantly improved mortality, increased body weight, and decreased markers of lung injury (Figure 1). Adoptive transfer was confirmed using flow cytometry to identify Tregs ($CD4^+Foxp3^+$ cells) or non-Tregs ($CD4^+Foxp3^-$ cells) in the BAL, lungs, and spleens of *Rag-1*$^{-/-}$ mice (*see* Figure E1 in the online supplement). These results confirm the critical role of Tregs in the normal resolution of LPS-induced lung injury, and establish the pattern of responses against which all other parameters are compared.

LPS-Induced Fibroproliferation Resolved in the Presence of Tregs

We assessed fibroproliferation by histology as well as by measuring collagen concentrations in the BAL and lungs of WT mice, *Rag-1*$^{-/-}$ mice, and *Rag-1*$^{-/-}$ mice that received Tregs or non-Treg $CD4^+$ cells. Collagen deposition and interstitial thickening were evident in both WT and *Rag-1*$^{-/-}$ mice on Day 3 after LPS injury. However, histologic changes resolved in WT mice by Day 7, whereas *Rag-1*$^{-/-}$ mice demonstrated persistent interstitial thickening and collagen deposition (Figure 2A). The adoptive transfer (AT) of Tregs but not non-Tregs into *Rag-1*$^{-/-}$ mice led to the histopathologic resolution of fibroproliferation (Figure 2B). Lung collagen concentrations (using the Sircol assay) increased in both WT and *Rag-1*$^{-/-}$ mice on Day 3, but remained persistently elevated in *Rag-1*$^{-/-}$ mice on Day 7 after LPS injury (Figure 2C). The AT of Tregs into *Rag-1*$^{-/-}$ mice reduced lung collagen concentrations to baseline by Day 7. Lung collagen remained significantly elevated in mice receiving non-Tregs, compared with both WT mice and mice that received Tregs. We also examined BAL fluid to see if collagen concentrations were altered in the alveolar compartment. WT and *Rag-1*$^{-/-}$ mice exhibited increased collagen in BAL fluid on Day 3 after LPS injury (Figure 2D). BAL collagen concentrations returned to baseline in WT mice, but remained elevated in *Rag-1*$^{-/-}$ mice up to Day 10 after LPS injury, compared with WT mice. The AT of Tregs, but not non-Tregs, into *Rag-1*$^{-/-}$ mice returned BAL collagen concentrations to baseline. BAL collagen was positively correlated with lung collagen, suggesting that fibroproliferation as measured in the alveolar compartment reflects overall lung fibroproliferation ($r = 0.73$, $P < 0.001$ by Pearson product moment correlation; Figure 2E). These data strongly support a vital role for Tregs in the resolution of fibroproliferation after LPS injury.

Tregs Reduced Lung and BAL Fibrocyte Number after ALI

Fibrocytes are circulating progenitor cells that can be recruited to sites of injury to become collagen-producing myofibroblasts. Fibrocytes can be identified according to the expression of the surface markers CD45 and CXCR4, and the intracellular expression of collagen-1 (Col-I) (12, 13) (Figure E2A). Using flow cytometry, we measured fibrocyte numbers in the lungs (Figure 3A) and BAL (Figure 3B) of WT and *Rag-1*$^{-/-}$ mice after LPS injury. Despite similar increases in both lung and BAL fibrocytes on Day 3 after LPS injury, fibrocytes were persistently elevated in *Rag-1*$^{-/-}$ mice compared with WT mice on Day 7. The AT of Tregs, but not non-Tregs, into *Rag-1*$^{-/-}$ mice returned both lung and BAL fibrocytes to WT concentrations. These results suggest that one of the mechanisms by which Tregs resolve fibroproliferation after LPS injury occurs through a reduction in lung fibrocyte number.

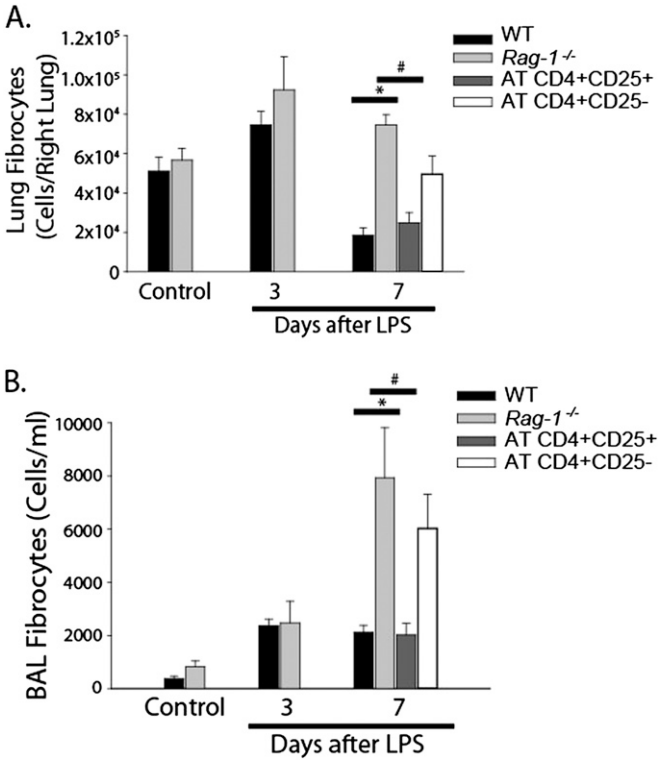

Figure 3. Fibrocytes were initially increased after LPS injury, and were reduced in the presence of Tregs. (*A*) Lung fibrocyte number was determined using flow cytometry to identify $CD45^+Col\text{-}1^+CXCR4^+$ cells in lung single-cell suspensions in all groups on Day 3 and Day 7 after intratracheal LPS ($^*P = 0.007$ and $^\#P = 0.017$, n ⩾ 6, all groups). (*B*) BAL fibrocyte number was determined using flow cytometry to identify $CD45^+Col\text{-}1^+CXCR4^+$ cells in BAL single-cell suspensions on Day 3 and Day 7 after intratracheal LPS ($^*P < 0.05$ and $^\#P < 0.05$, n ⩾ 4, all groups).

Epithelial-Derived CXCL12 Led to Fibrocyte Recruitment after LPS Injury

CXCL12 (or stromal cell-derived factor 1 [SDF-1]) is the most potent ligand for the CXCR4 receptor (expressed on fibrocytes), and is an important stimulus for fibrocyte recruitment to the lung after injury (12). We used immunohistochemistry to stain for CXCL12 in lung sections from WT and *Rag-1*$^{-/-}$ mice that had received either intratracheal water or LPS. CXCL12 was increased in both WT and *Rag-1*$^{-/-}$ mice on Day 3 after lung injury. On Day 7, CXCL12 returned to near baseline in WT mice, but *Rag-1*$^{-/-}$ mice demonstrated persistently elevated CXCL12 expression. At higher magnifications, epithelial cells appeared to comprise the predominant cell type that stained positive for CXCL12 after LPS injury (Figure 4A).

To confirm that epithelial cells were the major source of CXCL12 expression after LPS injury, we used multicolor flow cytometry to characterize intracellular CXCL12 expression in various cell populations in both WT and *Rag-1*$^{-/-}$ mice on Day 7 after LPS injury. We used biotinylated CD31 and CD45 antibodies with a V450-conjugated streptavidin to distinguish endothelial cells ($CD31^+$) and leukocytes ($CD45^+$) from other cell populations.

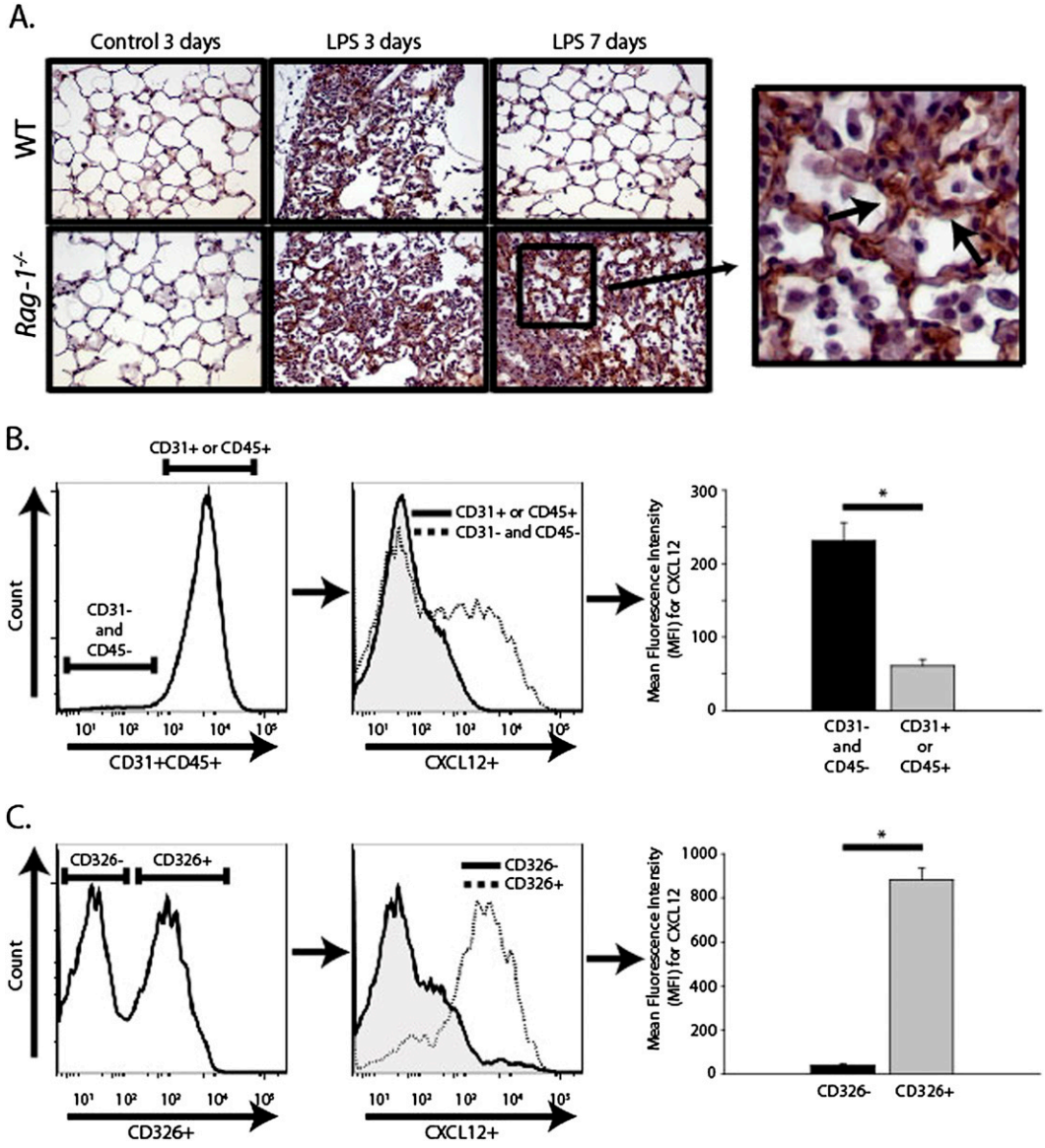

Figure 4. Epithelial cells were an important source of CXCL12 after LPS-induced lung injury. (*A*) Lung sections were stained for CXCL12 by immunohistochemistry on Day 3 and Day 7 after intratracheal LPS. Epithelial cells (*arrows*) appeared to be the predominant source of CXCL12 staining (images are of representative examples, ×200 magnification, $n \geqslant 2$ mice in each group; *inset*, ×400 magnification). (*B*) Single-cell suspensions were prepared from the lungs of WT and *Rag-1*$^{-/-}$ mice on Day 7 after intratracheal LPS or sterile water. Cells were stained with biotinylated anti-CD31 and anti-CD45, followed by V450-conjugated streptavidin as well as allophycocyanin-conjugated (APC)–Cy7–conjugated anti-CD326. Cells were fixed, permeabilized, and stained with APC-conjugated anti-CXCL12. Cells were gated for CD31 and CD45 positivity, and CXCL12 expression was examined by mean fluorescence intensity (MFI) (*$P < 0.001$, $n = 16$ mice). (*C*) CD31$^-$CD45$^-$ cells were gated for CD326 (epithelial cell adhesion molecule [EpCAM]) expression to identify epithelial cells. CXCL12 expression in CD326$^+$ and CD326$^-$ cells was examined by MFI (*$P < 0.001$, $n = 16$ mice).

CD31(−)CD45(−) cells exhibited a fourfold higher level of expression of CXCL12 by mean fluorescence intensity, suggesting that leukocytes and endothelial cells were not important sources of elevated lung CXCL12 expression after LPS injury (Figure 4B). Further examination of the CD31(−)CD45(−) cells revealed that the subset of cells that stained positive for the pan-epithelial marker, CD326, demonstrated a 22-fold higher level of CXCL12 expression compared with CD326-cells (Figure 4C). CD326, or epithelial cell adhesion molecule (EpCAM), was recently used to characterize human lung epithelial cell subsets (22). This provides strong evidence that epithelial cells were the primary source of the increased CXCL12 expression after LPS injury.

Tregs Reduced Lung CXCL12 Concentrations after LPS Injury

To better quantify CXCL12 expression and to determine the role of Tregs in the regulation of CXCL12 after LPS injury, we measured lung CXCL12 concentrations by ELISA in WT mice, *Rag-1*$^{-/-}$ mice, and *Rag-1*$^{-/-}$ mice that received Tregs and non-Treg CD4$^+$ lymphocytes. CXCL12 concentrations predicted lung fibrocyte numbers according to linear regression analysis ($r = 0.91$, $R^2 = 0.84$, $P < 0.001$; Figure 5A), consistent with the established role of CXCL12 as a chemokine for fibrocyte recruitment.

CXCL12 concentrations were significantly increased in both *Rag-1*$^{-/-}$ and WT mice on Day 3 after LPS injury (Figure 5B). CXCL12 concentrations returned to baseline by Day 7 in WT mice, but remained significantly elevated in *Rag-1*$^{-/-}$ mice. The AT of Tregs into *Rag-1*$^{-/-}$ mice reduced CXCL12 concentrations to baseline. The AT of non-Tregs into *Rag-1*$^{-/-}$ mice led to a slight reduction in CXCL12 concentrations, but CXCL12 remained significantly elevated compared with the *Rag-1*$^{-/-}$ control (92% higher), WT Day 7 LPS (80% higher), and AT Treg groups (45% higher). These data suggest that Tregs reduced the epithelial expression of CXCL12 after LPS injury, leading to decreased fibrocyte recruitment and the resolution of fibroproliferation.

Blockade of the CXCR4 Receptor with AMD3100 Decreased Fibroproliferation by Reducing Fibrocyte Recruitment to the Lung

To better understand the role of the CXCL12–CXCR4 axis in ALI fibroproliferation, we used the chemical AMD3100 to block the CXCR4 receptor. AMD3100 is a nonpeptide

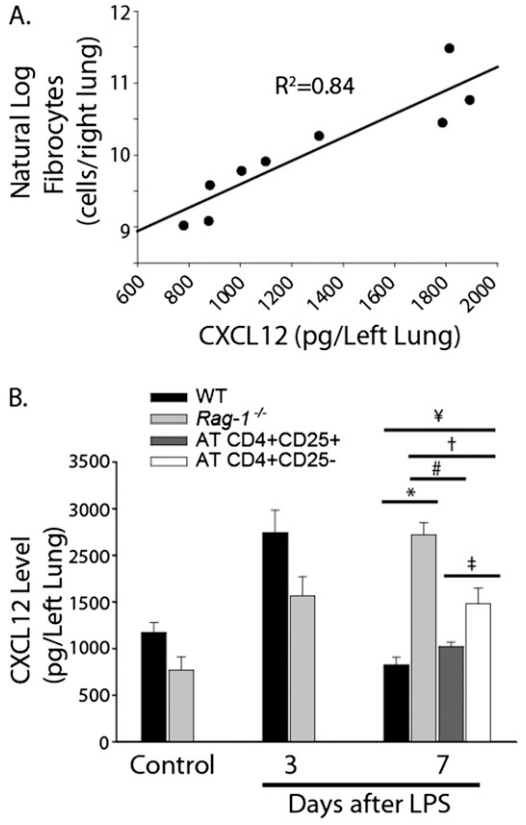

Figure 5. Adoptive transfer of Tregs reduced lung CXCL12 concentrations. CXCL12 concentrations were measured in whole-lung homogenates by ELISA. (*A*) CXCL12 concentrations were positively correlated with the natural log of lung fibrocyte numbers ($r = 0.91$, $R^2 = 0.84$, $P < 0.001$, using linear regression on log-transformed data; $n = 9$ total mice where CXCL12 concentrations and lung fibrocyte numbers were available from the same time point: 5 *Rag-1*$^{-/-}$ AT non-Tregs, 3 *Rag-1*$^{-/-}$ AT-Tregs, and 1 WT Day 7 LPS). (*B*) CXCL12 concentrations were determined by ELISA on whole-lung homogenates on Day 3 and day 7 after intratracheal LPS ($^{*}P < 0.001$, $^{\#}P < 0.001$, $^{\dagger}P = 0.009$, $^{¥}P = 0.01$, and $^{\ddagger}P = 0.036$, n ⩾ 4, all groups).

antagonist of CXCR4 that inhibits the binding and function of CXCL12 with high affinity and specificity (23, 24). *Rag-1*$^{-/-}$ mice received intratracheal LPS on Day 0, followed by daily intraperitoneal injections of either AMD3100 (200 μg in 250 μl) or sterile PBS (250 μl), starting on Day 0. Mortality was no different between *Rag-1*$^{-/-}$ mice that received AMD3100 and *Rag-1*$^{-/-}$ mice that received PBS (25% and 27%, respectively). Peak weight loss was measured at nearly 25% of initial body weight in both groups, and was similar to the peak weight loss observed in WT and *Rag-1*$^{-/-}$ mice that received LPS alone (Figure 6A). BAL protein and cell counts were not significantly different between groups (Figure E4). In *Rag-1*$^{-/-}$ mice, CXCR4 receptor blockade with AMD3100 decreased lung fibrocytes (Figure 6B), histologic fibrosis (Figure 6C), and lung collagen (Figure 6D) on Day 7 after intratracheal LPS. Lung CXCL12 concentrations were no different between *Rag-1*$^{-/-}$ mice that received AMD3100 or PBS (Figure 6E), indicating that the difference in fibrocyte numbers between groups was attributable to the CXCR4 receptor blockade rather than a decrease in CXCL12 expression. WT animals receiving intratracheal LPS and daily injections of AMD3100 did not exhibit reduced inflammation on Day 4 after lung injury, as measured by BAL protein (Figure E4A) and cell count (Figure E4B), demonstrating that AMD3100 does not markedly alter the inflammatory response to LPS. These results provide further evidence that fibrocytes recruited along the CXCL12–CXCR4 axis play an important role in fibroproliferation after LPS injury, because blocking CXCR4 reduces fibrocyte numbers, collagen deposition, and fibrosis in *Rag-1*$^{-/-}$ mice.

DISCUSSION

Fibroproliferation is part of the normal repair response to ALI (5). This repair begins early, as evidenced by increased markers of collagen turnover in the BAL fluid of patients with ARDS within the first days of diagnosis (25, 26). However, excessive fibroproliferation is associated with worse outcomes, because patients develop decreased lung compliance and increased dead space, and require prolonged mechanical ventilation (4, 6, 8). Despite its importance to patient outcomes, the factors that underlie fibroproliferation in ALI remain poorly understood.

Tregs down-regulate lung inflammation in a number of contexts (27–30). Because the fibroproliferative phase of ARDS is characterized by persistent interstitial inflammation (4), Tregs might be expected to reduce fibroproliferation, perhaps by dampening the inflammation that leads to myofibroblast accumulation and collagen deposition (31). Patients with IPF and collagen vascular disease–associated pulmonary fibrosis demonstrate a reduced number and function of Tregs in BAL fluid and peripheral blood, compared with controls, suggesting that Tregs may play a role in fibroproliferation (27). However, conflicting data in the literature have emerged regarding Tregs in animal models of pulmonary fibrosis (31–34), suggesting that the role of Tregs in regulating fibroproliferation may be both context-specific and site-specific. To our knowledge, the role of Tregs in the fibroproliferative response to ALI has not been described.

Our data support a novel role for Tregs in accelerating the resolution of fibroproliferation by decreasing fibrocyte recruitment to the lung after injury. Fibrocytes are CD45^{+}Col-1^{+}CXCR4^{+} bone marrow–derived cells that migrate to sites of injury to become collagen-producing myofibroblasts (12, 13). Fibrocytes play an important role in bleomycin models of pulmonary fibrosis (10, 15). They are present in the BAL fluid and blood of patients with IPF, and increased fibrocyte numbers predict exacerbations (14, 16). Fibrocytes are also found in the BAL fluid of patients with ARDS, and are associated with increased mortality (17, 18).

CXCL12 is constitutively expressed in a number of tissues, and binds to the CXCR4 receptor on fibrocytes to promote migration (12, 14, 35–37). The significant association between lung CXCL12 concentrations and fibrocyte numbers in our model supports previous studies that demonstrated the importance of CXCL12 in fibrocyte recruitment (12, 13). CXCL12 secretion is induced in rat Type II epithelial cells after scratch injury, implicating the epithelium as an important source of CXCL12 (38). In patients with IPF, epithelial cells expressed CXCL12 at higher concentrations than in control samples (14). Epithelial CXCL12 increases in both murine and human lungs after ALI (39). Our data indicate that CD326^{+} epithelial cells are the most abundant source of CXCL12 expression after LPS-induced ALI.

Our study shows that Tregs facilitate the resolution of ALI fibroproliferation by decreasing lung CXCL12 concentrations, leading to a reduction in lung fibrocytes and a decrease in collagen deposition and fibrosis. Tregs might alter lung CXCL12 concentrations in a number of ways. Because epithelial cells are the most abundant source of CXCL12 after LPS injury, Tregs likely modulate epithelial CXCL12 expression. Treg–epithelial interactions were previously described. For example, crosstalk between Tregs and the intestinal or retinal epithelium is an

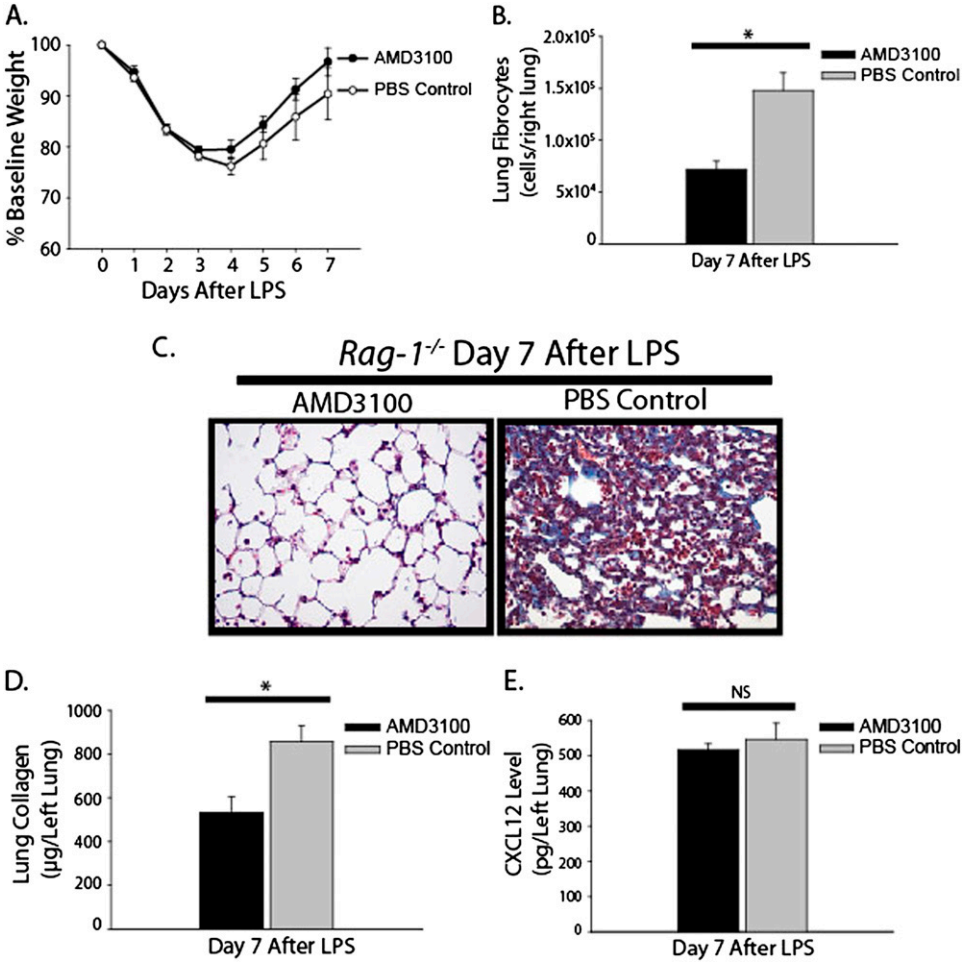

Figure 6. Blockade of the CXCR4 receptor with AMD3100 reduced fibroproliferation in *Rag-1*$^{-/-}$ mice by reducing fibrocyte recruitment to the lung after LPS injury. (*A*) Weight loss presented as percentage of baseline weight after intratracheal LPS for *Rag-1*$^{-/-}$ mice that received intraperitoneal AMD3100 or intraperitoneal PBS. (*B*) Lung fibrocyte number was determined using flow cytometry to identify CD45^{+}Col-1^{+} CXCR4^{+} cells in lung single-cell suspensions in both groups on Day 7 after intratracheal LPS (*$P = 0.001$; n $\geq$ 7, all groups). (*C*) Lung sections were stained with Masson's trichrome to highlight collagen deposition on Day 7 after intratracheal LPS in both groups (images are of representative examples; magnification, $\times$200). (*D*) Lung collagen was measured by Sircol assay in both groups on Day 7 after intratracheal LPS (*$P = 0.012$; n $\geq$ 5, all groups). (*E*) CXCL12 concentrations were measured in whole-lung homogenates by ELISA in both groups on Day 7 after intratracheal LPS (n $\geq$ 5, all groups).

important determinant of both immune tolerance and Treg proliferation (40–42). Type II alveolar epithelial cells (AECs) can present antigen to naive Tcells through the Class II major histocompatibility complex (MHC), and induce the proliferation of Tregs, in part through a transforming growth factor (TGF)–β–dependent mechanism (43). In the context of our model, Tregs might down-regulate AEC CXCL12 expression in a contact-dependent manner. For example, the engagement of Class II MHC receptors on epithelial cells by Tregs might lead to a change in CXCL12 expression. Furthermore, a contact-independent interaction might occur between Tregs and AECs, perhaps through the release of cytokines that decrease AEC CXCL12 production. Tregs may also exert their effects on AECs through a third cell type. For example, our group has shown that Tregs decrease the macrophage production of TNF-α in a contact-dependent manner (19). An alteration in macrophage phenotype might then lead to a decrease in AEC CXCL12 production. Future experiments will seek to identify the specific interactions between Tregs and epithelial cells that govern overall CXCL12 expression and subsequent fibrocyte recruitment in the context of ALI.

The reduction in lung collagen concentrations and fibrocytes in *Rag-1*$^{-/-}$ mice after CXCR4 receptor blockade with AMD3100 provides further evidence that the CXCL12–CXCR4 axis is critical in fibrocyte-mediated ALI fibroproliferation, and is consistent with previous studies that demonstrated a reduction in lung fibrosis in bleomycin models after CXCR4 or CXCL12 blockade (12, 24). The lack of a significant difference in BAL cell count, protein, and lung CXCL12 concentrations between AMD3100-treated *Rag-1*$^{-/-}$ mice and PBS control mice, as well as the similar peak weight loss in each group, indicate that the difference in fibroproliferation did not result from reduced inflammation after LPS injury, and was instead attributable to the decrease in fibrocyte number. The uncoupling of inflammation and fibroproliferation in this context further supports the notion that the reduction in fibroproliferation seen in our Treg AT experiments was not solely the result of a Treg-dependent decrease in inflammation, but was in part attributable to a reduction in fibrocyte recruitment. Given the potential difficulties of using Tregs as therapy for human autoimmune and inflammatory diseases (44), the pharmacologic manipulation of downstream pathways such as the CXCL12–CXCR4 axis may provide attractive targets for ALI treatment in the future.

Factors in addition to fibrocyte recruitment along the CXCL12–CXCR4 axis likely modulate fibrocyte numbers and subsequent fibroproliferation in the context of ALI. For example, Tregs could influence both fibrocyte proliferation and survival. Moreover, fibrocyte number alone clearly does not explain the differences in lung collagen concentrations seen between our experimental groups, as evidenced by the finding that lung fibrocytes were lower in WT mice on Day 7 after LPS compared with water control mice, yet lung collagen concentrations were slightly higher in the Day 7 WT mice. The collagen-producing capacity of fibrocytes likely depends in part on their surrounding environment. In addition, our flow cytometry markers may not have identified fibrocytes as they transitioned to a myofibroblast phenotype. In culture, fibrocytes lose the expression of CD34 and CD45 as they transition to a collagen-producing cell (45), making them potentially difficult to track once they transition to a myofibroblast phenotype *in vivo*. Future

experiments will seek to examine differences in fibrocyte proliferation, survival, and collagen-producing capacity in the context of ALI fibroproliferation, and to refine the tracking of fibrocytes after they transition to a myofibroblast phenotype.

Our study contains other important limitations. Although the purity of our bead-sorted Tregs used in adoptive transfers was consistently greater than 85%, some $CD4^{-}CD25^{+}$ cells were included in our ATs. Although these represented on average less than 7.5% of overall transferred cells, they may have contributed to the reduction in fibroproliferation. In addition to Tregs, CD25 can be expressed in $CD8^{+}$ T cells, activated B cells, and (at lower concentrations) monocytes. Almost all of the $CD4^{-}CD25^{+}$ cells demonstrated a low forward and side scatter by flow cytometry, suggesting they were likely lymphocytes (data not shown). Our group has shown that the AT of splenocytes from CD4-depleted spleens into *Rag-1*$^{-/-}$ mice does not resolve LPS-induced lung injury. Furthermore, the AT of $CD8^{+}$ lymphocytes into *Rag-1*$^{-/-}$ mice dose not result in the resolution of lung injury (19). This suggests that $CD4^{-}CD25^{+}$ cells do not play a role in reducing fibroproliferation in our model. Treg depletion with the CD25-specific antibody PC61 impairs the resolution of lung injury, further emphasizing the critical role of Tregs in our model of lung injury (19).

The small but significant decrease in CXCL12 concentrations after the AT of non-Tregs into *Rag-1*$^{-/-}$ mice might suggest that $CD4^{+}$ lymphocytes other than Tregs play a role in reducing fibroproliferation. However, this small reduction in CXCL12 did not result in decreased biochemical or histologic markers of fibroproliferation. The decrease in CXCL12 may also have been the result of a small number of Tregs present in the non-Treg ATs, either from bead separation impurities or from the induction of naive $CD4^{+}$ lymphocytes into Tregs (46). Although we did not find significant numbers of Tregs in the lungs of *Rag-1*$^{-/-}$ mice that received non-Tregs on Day 7 after AT, the number of Tregs required to reduce CXCL12 concentrations and the kinetics of this response remain unknown.

Although our study highlighted an important role for fibrocytes in ALI fibroproliferation, it did not address the potential contributions of other cell types to the activated myofibroblast pool. Resident fibroblasts were shown to be an important source of collagen deposition and fibrosis in both animal and human models. Recently an interest has emerged in the concept of epithelial-to-mesenchymal transition, whereby epithelial cells may either transform into collagen-producing myofibroblasts or secrete profibrotic growth factors and cytokines that can lead to fibroproliferation (10, 47). Future experiments will seek to define the role of these cell types in our injury model.

In conclusion, we report on a unique role for Tregs in the resolution of ALI fibroproliferation through the control of fibrocyte recruitment to the lung after LPS injury. A better understanding of the role of Tregs in the fibroproliferative response will potentially uncover pathways that might lead to new diagnostic and therapeutic options in patients with ALI.

Author disclosures are available with the text of this article at www.atsjournals.org.

Acknowledgments: The authors thank James Watkins and Andre Robinson at the Johns Hopkins Pulmonary Histology Core, Allen Myers at the Johns Hopkins Bayview Immunohistochemistry Core, and Joe Chrest and Mark Soloski at the Johns Hopkins Bayview Flow Cytometry Core.

References

1. Rubenfeld GD, Caldwell E, Peabody E, Weaver J, Martin DP, Neff M, Stern EJ, Hudson LD. Incidence and outcomes of acute lung injury. *N Engl J Med* 2005;353:1685–1693.
2. The Acute Respiratory Distress Syndrome Network. Ventilation with lower tidal volumes as compared with traditional tidal volumes for acute lung injury and the acute respiratory distress syndrome. *N Engl J Med* 2000;342:1301–1308.
3. Phua J, Badia JR, Adhikari NKJ, Friedrich JO, Fowler RA, Singh JM, Scales DC, Stather DR, Li A, Jones A, *et al*. Has mortality from acute respiratory distress syndrome decreased over time? A systematic review. *Am J Respir Crit Care Med* 2009;179:220–227.
4. Ware LB, Matthay MA. The acute respiratory distress syndrome. *N Engl J Med* 2000;342:1334–1349.
5. Meduri GU, Chinn AJ, Leeper KV, Wunderink RG, Tolley E, Winer-Muram HT, Khare V, Eltorky M. Corticosteroid rescue treatment of progressive fibroproliferation in late ARDS: patterns of response and predictors of outcome. *Chest* 1994;105:1516–1527.
6. Zapol WM, Trelstad RL, Coffey JW, Tsai I, Salvador RA. Pulmonary fibrosis in severe acute respiratory failure. *Am Rev Respir Dis* 1979; 119:547–554.
7. Martin C, Papazian L, Payan M, Saux P, Gouin F. Pulmonary fibrosis correlates with outcome in adult respiratory distress syndrome. *Chest* 1995;107:196–200.
8. Ichikado K, Suga M, Muranaka H, Gushima Y, Miyakawa H, Tsubamoto M, Johkoh T, Hirata N, Yoshinaga T, Kinoshita Y, *et al*. Prediction of prognosis for acute respiratory distress syndrome with thin-section CT: validation in 44 cases. *Radiology* 2006;238:321–329.
9. McAnulty RJ, Campa JS, Cambrey AD, Laurent GJ. The effect of transforming growth factor [beta] on rates of procollagen synthesis and degradation *in vitro*. *Biochim Biophys Acta* 1991;1091:231–235.
10. Tanjore H, Xu XC, Polosukhin VV, Degryse AL, Li B, Han W, Sherrill TP, Plieth D, Neilson EG, Blackwell TS, *et al*. Contribution of epithelial-derived fibroblasts to bleomycin-induced lung fibrosis. *Am J Respir Crit Care Med* 2009;180:657–665.
11. Kim KK, Wei Y, Szekeres C, Kugler MC, Wolters PJ, Hill ML, Frank JA, Brumwell AN, Wheeler SE, Kreidberg JA, *et al*. Epithelial cell alpha3-beta1 integrin links beta-catenin and SMAD signaling to promote myofibroblast formation and pulmonary fibrosis. *J Clin Invest* 2009;119:213–224.
12. Phillips RJ, Burdick MD, Hong K, Lutz MA, Murray LA, Xue YY, Belperio JA, Keane MP, Strieter RM. Circulating fibrocytes traffic to the lungs in response to CXCL12 and mediate fibrosis. *J Clin Invest* 2004;114:319–321.
13. Strieter RM, Keeley EC, Hughes MA, Burdick MD, Mehrad B. The role of circulating mesenchymal progenitor cells (fibrocytes) in the pathogenesis of pulmonary fibrosis. *J Leukoc Biol* 2009;86:1111–1118.
14. Andersson-Sjoland A, de Alba CG, Nihlberg K, Becerril C, Ramirez R, Pardo A, Westergren-Thorsson G, Selman M. Fibrocytes are a potential source of lung fibroblasts in idiopathic pulmonary fibrosis. *Int J Biochem* 2008;40:2129–2140.
15. Hashimoto N, Jin H, Liu T, Chensue SW, Phan SH. Bone marrow-derived progenitor cells in pulmonary fibrosis. *J Clin Invest* 2004;113:243–252.
16. Moeller A, Gilpin SE, Ask K, Cox G, Cook D, Gauldie J, Margetts PJ, Farkas L, Dobranowski J, Boylan C, *et al*. Circulating fibrocytes are an indicator of poor prognosis in idiopathic pulmonary fibrosis. *Am J Respir Crit Care Med* 2009;179:588–594.
17. Quesnel C, Piednoir P, Nardelli L, Garnier M, Leçon V, Lasocki S, Bouadma L, Elbim C, Mentré F, Dehoux M. Alveolar fibrocyte percentage is an independent predictor of poor outcome in patients with acute lung injury. *Crit Care Med* 2012;40:21–28.
18. Quesnel C, Nardelli L, Piednoir P, Lecon V, Marchal-Somme J, Lasocki S, Bouadma L, Philip I, Soler P, Crestani B, *et al*. Alveolar fibroblasts in acute lung injury: biological behaviour and clinical relevance. *Eur Respir J* 2010;35:1312–1321.
19. D'Alessio FR, Tsushima K, Aggarwal NR, West EE, Willett MH, Britos MF, Pipeling MR, Brower RG, Tuder RM, McDyer JF, *et al*. $CD4^{+}CD25^{+}Foxp3^{+}$ Tregs resolve experimental lung injury in mice and are present in humans with acute lung injury. *J Clin Invest* 2009;119:2898–2913.
20. Matute-Bello G, Downey G, Moore BB, Groshong SD, Matthay MA, Slutsky AS, Kuebler WM, on behalf of the Acute Lung Injury in Animals Study Group. An official American Thoracic Society workshop report: features and measurements of experimental acute lung injury in animals. *Am J Respir Cell Mol Biol* 2011;44:725–738.
21. Garibaldi B, D'Alessio F, Files DC, Chau E, Sidhaye V, Fraig M, King LS. Regulatory T-lymphocytes play a key role in the fibroproliferative response to acute lung injury [abstract]. *Am J Respir Crit Care Med* 2010;181:A3772.
22. Fujino N, Kubo H, Ota C, Suzuki T, Suzuki S, Yamada M, Takahashi T, He M, Suzuki T, Kondo T, *et al*. A novel method for isolating individual cellular components from the adult human distal lung. *Am J Respir Cell Mol Biol* 2012;46:422–430.

23. Rosenkilde MM, Gerlach LO, Jakobsen JS, Skerlj RT, Bridger GJ, Schwartz TW. Molecular mechanism of AMD3100 antagonism in the CXCR4 receptor. *J Biol Chem* 2004;279:3033–3041.
24. Song JS, Kang CM, Kang HH, Yoon HK, Kim YK, Kim KH, Moon HS, Park SH. Inhibitory effect of CXC chemokine receptor 4 antagonist AMD3100 on bleomycin induced murine pulmonary fibrosis. *Exp Mol Med* 2010;42:465–476.
25. Armstrong L, Thickett DR, Mansell JP, Ionescu M, Hoyle E, Billinghurst R, Poole R, Millar AB. Changes in collagen turnover in early acute respiratory distress syndrome. *Am J Respir Crit Care Med* 1999;160: 1910–1915.
26. Marshall RP, Bellingan G, Webb S, Puddicombe A, Goldsack N, McAnulty RJ, Laurent GJ. Fibroproliferation occurs early in the acute respiratory distress syndrome and impacts on outcome. *Am J Respir Crit Care Med* 2000;162:1783–1788.
27. Kotsianidis I, Nakou E, Bouchliou I, Tzouvelekis A, Spanoudakis E, Steiropoulos P, Sotiriou I, Aidinis V, Margaritis D, Tsatalas C, *et al*. Global impairment of $CD4^+CD25^+FOXP3^+$ regulatory T cells in idiopathic pulmonary fibrosis. *Am J Respir Crit Care Med* 2009;179: 1121–1130.
28. Hartl D, Koller B, Mehlhorn AT, Reinhardt D, Nicolai T, Schendel DJ, Griese M, Krauss-Etschmann S. Quantitative and functional impairment of pulmonary $CD4^+CD25^{hi}$ regulatory T cells in pediatric asthma. *J Allergy Clin Immunol* 2007;119:1258–1266.
29. Tosiek MJ, Gruber AD, Bader SR, Mauel S, Hoymann HG, Prettin S, Tschernig T, Buer J, Gereke M, Bruder D. $CD4^+CD25^+Foxp3^+$ regulatory T cells are dispensable for controlling $CD8^+$ T cell–mediated lung inflammation. *J Immunol* 2011;186:6106–6118.
30. Schreiber TH, Wolf D, Tsai MS, Chirinos J, Deyev VV, Gonzalez L, Malek TR, Levy RB, Podack ER Therapeutic Treg expansion in mice by TNFRSF25 prevents allergic lung inflammation. *J Clin Invest* 2010; 120:3629–3640.
31. Wilson MS, Wynn TA. Pulmonary fibrosis: pathogenesis, etiology and regulation. *Mucosal Immunol* 2009;2:103–121.
32. Trujillo G, Hartigan A, Hogaboam C. T regulatory cells and attenuated bleomycin-induced fibrosis in lungs of $CCR7^{-/-}$ mice. *Fibrogenesis Tissue Repair* 2010;3:18.
33. Boveda-Ruiz D, Alessandro-Gabazza CN, Toda M, Takagi T, Naito M, Matsushima Y, Matsumoto T, Kobayashi T, Gil-Bernabe P, Chelakkot-Govindalayathil AL, *et al*. Differential role of regulatory T cells in early and late stages of pulmonary fibrosis. *Immunobiology* (In press)
34. Lo Re S, Lecocq M, Uwambayinema F, Yakoub Y, Delos M, Demoulin JB, Lucas S, Sparwasser T, Renauld JC, Lison D, *et al*. PDGF-producing $CD4^+$ $Foxp3^+$ regulatory T lymphocytes promote lung fibrosis. Am J Respir Crit Care Med 2011;184:1270–1281.
35. Santiago B, Calonge E, Rey MJD, Gutierrez-Canas I, Izquierdo E, Usategui A, Galindo M, Alcami J, Pablos JL. CXCL12 gene expression is upregulated by hypoxia and growth arrest but not by inflammatory cytokines in rheumatoid synovial fibroblasts. *Cytokine* 2011;53:184–190.
36. Karin N. The multiple faces of CXCL12 (SDF-1) in the regulation of immunity during health and disease. *J Leukoc Biol* 2010;88:463–473.
37. Reilkoff RA, Bucala R, Herzog EL. Fibrocytes: emerging effector cells in chronic inflammation. *Nat Rev Immunol* 2011;11:427–435.
38. Ghosh MC, Makena PS, Gorantla VK, Sinclair SE, Waters CM. CXCR4 regulates migration of lung alveolar epithelial cells through activation of Rac1 and matrix metalloproteinase–2 (MMP-2). *Am J Physiol Lung Cell Mol Physiol* 2012;302:L846–L856.
39. Petty JM, Sueblinvong V, Lenox CC, Jones CC, Cosgrove GP, Cool CD, Rai PR, Brown KK, Weiss DJ, Poynter ME, *et al*. Pulmonary stromal–derived factor–1 expression and effect on neutrophil recruitment during acute lung injury. *J Immunol* 2007;178:8148–8157.
40. Chen X, Song CH, Feng BS, Li TL, Li P, Zheng PY, Chen XM, Xing Z, Yang PC. Intestinal epithelial cell–derived integrin AB6 plays an important role in the induction of regulatory T cells and inhibits an antigen-specific Th2 response. *J Leukoc Biol* 2011;90:751–759.
41. Beswick EJ, Pinchuk IV, Earley RB, Schmitt DA, Reyes VE. Role of gastric epithelial cell–derived transforming growth factor beta in reduced $CD4^+$ T cell proliferation and development of regulatory T cells during *Helicobacter pylori* infection. *Infect Immun* 2011;79:2737–2745.
42. Kawazoe Y, Sugita S, Keino H, Yamada Y, Imai A, Horie S, Mochizuki M. Retinoic acid from retinal pigment epithelium induces T regulatory cells. *Exp Eye Res* 2012;94:32–40.
43. Gereke M, Jung S, Buer J, Bruder D. Alveolar Type II epithelial cells present antigen to $CD4^+$ T Cells and induce $Foxp3^+$ regulatory T cells. *Am J Respir Crit Care Med* 2009;179:344–355.
44. Riley JL, June CH, Blazar BR, Human T. Regulatory cell therapy: take a billion or so and call me in the morning [abstract]. *Immunity* 2009; 30:656–665.
45. Mori L, Bellini A, Stacey MA, Schmidt M, Mattoli S. Fibrocytes contribute to the myofibroblast population in wounded skin and originate from the bone marrow. *Exp Cell Res* 2005;304:81–90.
46. Josefowicz SZ, Rudensky A. Control of regulatory T cell lineage commitment and maintenance. *Immunity* 2009;30:616–625.
47. Laurent M, Hill M, Chambers R. Escape from the matrix: multiple mechanisms for fibroblast activation in pulmonary fibrosis. *Proc Am Thorac Soc* 2008;5:311–315.